Views and Reviews

Susceptibility-Weighted Imaging of the Brain: Current Utility and Potential Applications

Richard J. Robinson, MBChB, Sandeep Bhuta, MBBS, DMRD, DNB, FRANZCR

From Griffith University, School of Medicine, Department of Medical Imaging, Gold Coast Hospital, Queensland 4215, Australia.

ABSTRACT

BACKGROUND AND PURPOSE

Susceptibility-Weighted Imaging (SWI) is a relatively new magnetic resonance imaging (MRI) sequence relying on susceptibility differences between adjacent tissues to produce an image. It is extremely sensitive for detection of blood products (hemosiderin, ferritin), deoxygenated blood, calcium, iron, and small vein depiction. Little information is available in the literature to describe common findings seen using this imaging sequence. This article is an comprehensive review of appearances across the spectrum of brain pathology encountered in routine clinical practice.

MATERIALS AND METHODS

A retrospective review of 400 MRI Brain examinations was performed by one fellowship trained Neuroradiologist with 5 years experience (SB) and one general radiologist (RR). Agreement was by consensus observing normal and pathological imaging features seen in SWI sequences.

RESULTS

Results are presented as a comprehensive pictorial review highlighting the key imaging findings observed and new directions using SWI.

CONCLUSION

SWI is an extremely useful adjunct to current MRI sequences of the brain and is advocated for inclusion into routine Neuroimaging protocols.

Keywords: Susceptibility-Weighted Imaging; Cerebrovascular disease; Traumatic brain injury; Venous Sinus Thrombosis; Minimum Intensity Projection; Cerebrospinal fluid; Fluid attenuated inversion recovery; Magnetic Resonance Imaging; Diffuse axonal injury; Computed Tomography; Subdural Hematoma; Subarachnoid Hemorrhage; Cerebral amyloid angiopathy; Cerebral autosomal dominant arteriopathy with subcortical infarcts and leukoencephalopathy; Developmental Venous Anomalies; Neurodegeneration with brain iron accumulation; Pantothenate kinase associated neurodegeneration; Multiple Sclerosis; Glioblastoma Multiforme; World Health Organization.

Acceptance: Received September 27, 2009, and in revised form May 27, 2010. Accepted for publication July 15, 2010.

Correspondence: Address correspondence to Sandeep Bhuta, MBBS, DNB, FRANZCR, Associate Professor of Radiology, Griffith University, School of Medicine, Department of Medical Imaging, 108 Nerang Street, Gold Coast Hospital, Gold Coast, QLD, 4215, Australia. E-mail: sandeepbhuta@gmail.com.

J Neuroimaging 2011;21:e189-e204.
DOI: 10.1111/j.1552-6569.2010.00516.x

Introduction

Susceptibility-weighted imaging (SWI) is a relatively new magnetic resonance imaging (MRI) sequence that has been advocated for use in a number of clinical applications.[1,2] It utilizes the susceptibility differences between adjacent tissues to produce tissue contrast and is extremely sensitive in the detection of diamagnetic and paramagnetic substances such as blood products (hemeosiderin and ferritin), deoxygenated blood, calcium, iron, and small vein depiction. Some of the findings described maybe seen on conventional T2* images but SWI offers enhanced sensitivity and depicts blood products and calcium better then gradient echo (GRE) sequences.

Since its introduction, we have found that SWI offers additional diagnostic information across a wide spectrum of brain pathology including cerebrovascular disease (CVD), traumatic brain injury (TBI), neurodegenerative disorders, venous sinus thrombosis (VST), cerebral microhemorrhages, demyelination, cerebral neoplasia, and intracranial hemorrhage. SWI also enables the differentiation of calcium from blood products. The full utility of SWI has yet to be validated in the medical literature; however, we believe SWI offers diagnostic benefit over and above current imaging sequences in many of the above conditions. This article presents our experience in using SWI highlighting cases in which diagnostic specificity was improved

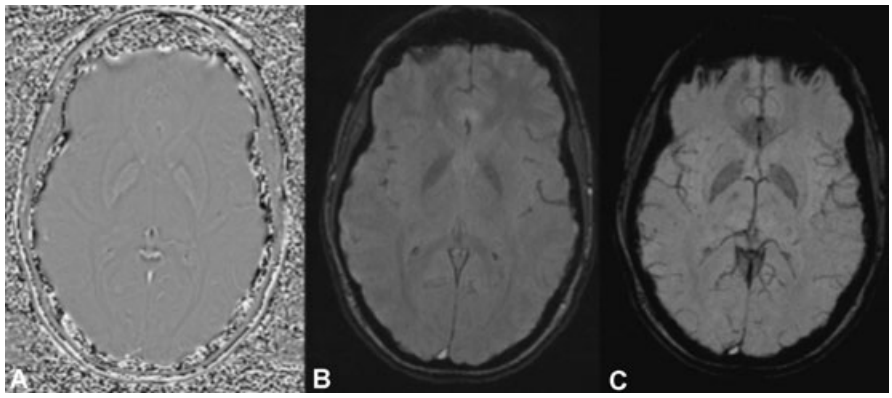

Fig 1. (A–C) Corresponding axial phase, magnitude, and final SWI images. The phase and final SWI image are used for diagnostic purposes.

and areas that we feel SWI may offer future benefit reliant on appropriate good quality research.

Materials and Methods

Background Physics

A full description of the physics behind SWI has been discussed in detail by other authors[3] and is beyond the scope of this article. Typical MRI sequences utilize magnitude data to produce tissue contrast. In SWI, a gradient echo sequence is utilized with TR and TE values set to produce an image somewhere between T1 and T2 weighting. The magnitude image is produced as in any normal MRI sequence. Phase data have historically been discarded as any useful information was obscured by background magnetic field inhomogeneity. Development of sophisticated phase filters has enabled removal of unwanted phase artefacts producing useful soft tissue contrast and a usable image. Multiplying the phase and magnitude data sets produces the final SWI image used for diagnostic purposes. This process is performed automatically by the MRI console and is presented as a Minimum Intensity Projection (MNIP). This MNIP can then be processed to produce a more conventional axial image correlating to 4-mm Slice thickness. The combination of magnitude and phase information provides the exquisite sensitivity for susceptibility effect. Display of the phase image is also required to allow complete interpretation of the sequence; this is discussed below.

Normal SWI Appearances

Importance of Phase Images

Review of the final SWI image and the separate phase image is required for accurate interpretation (see Fig 1). The phase image allows differentiation between paramagnetic (eg, blood products) and diamagnetic substances (eg, calcium). Subtle differences exist between the phase images produced by the systems of different manufacturers. Identification of the system

Table 1. Phase Signal Characteristics in Left- and Right-Handed MRI Systems

	Right-Handed System (RHS) (eg, GE)	Left-Handed System (LHS) (eg, Siemens)
Paramagnetic phase image signal (eg, hemosiderin)	Dark	Bright
Diamagnetic phase image signal (eg, calcium)	Bright	Dark

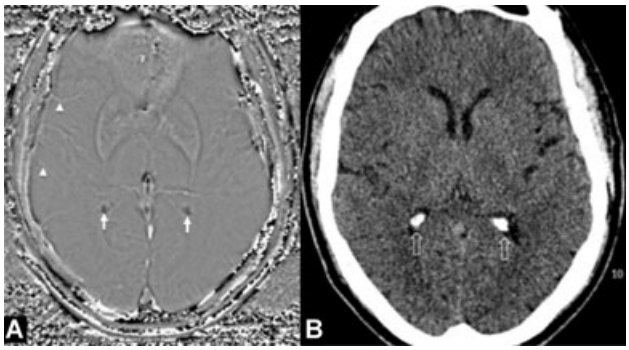

Fig 2. (A) An axial phase image revealing low signal choroid plexus (arrows) corresponding to negative phase shift. This indicates a diamagnetic substance. Increased signal is seen in the cortical veins (arrowheads) indicating a positive phase shift induced by paramagnetic deoxyhemoglobin. (B) The corresponding CT examination demonstrating choroid plexus calcification (open arrow).

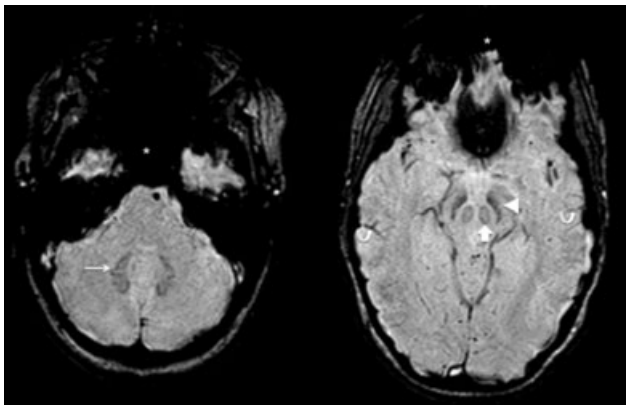

Fig 3. Normal anatomy as depicted on the final SWI image. The dentate nucleus (arrow), cortical veins (curved arrow), red nucleus (block arrow), and pars compacta of the substantia nigra (arrowhead) are all demonstrated. Dephasing artefact caused by the skull is seen as low signal (asterix).

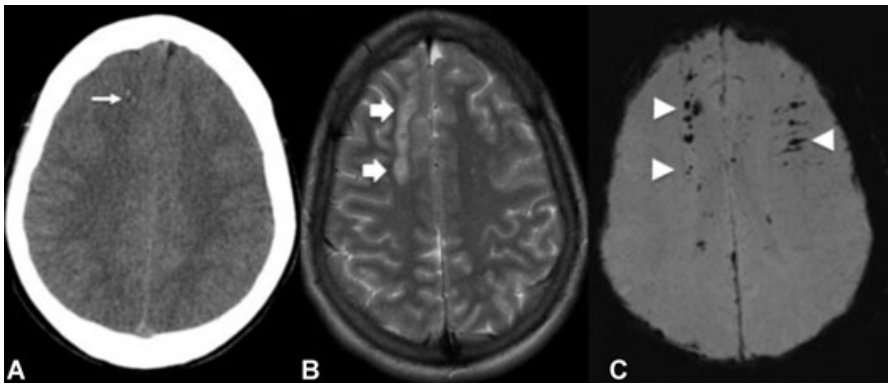

Fig 4. Taken from a patient with traumatic brain injury following a motor vehicle accident. CT examination (A) reveals a small amount of hemorrhagic contusion in the right frontal lobe (arrow). (B) The corresponding T2-weighted MRI revealing more extensive injury within the right frontal lobe. The SWI sequence (C) reveals the full distribution of injury with the demonstration of hemorrhagic foci in both frontal lobes (arrowheads). The linear pattern in the left frontal lobe is consistent with shearing effect seen in diffuse axonal injury.

Fig 5. Fifty-six-year-old male presenting with a suspected posterior fossa stroke. (A) (Axial) and (B) (coronal) SWI sequences revealing low signal susceptibility effect in the left vertebral artery corresponding to in situ thrombus. (C) (Axial phase) reveals corresponding high signal indicating paramagnetic thrombus (D) taken from the contrast-enhanced carotid angiogram.

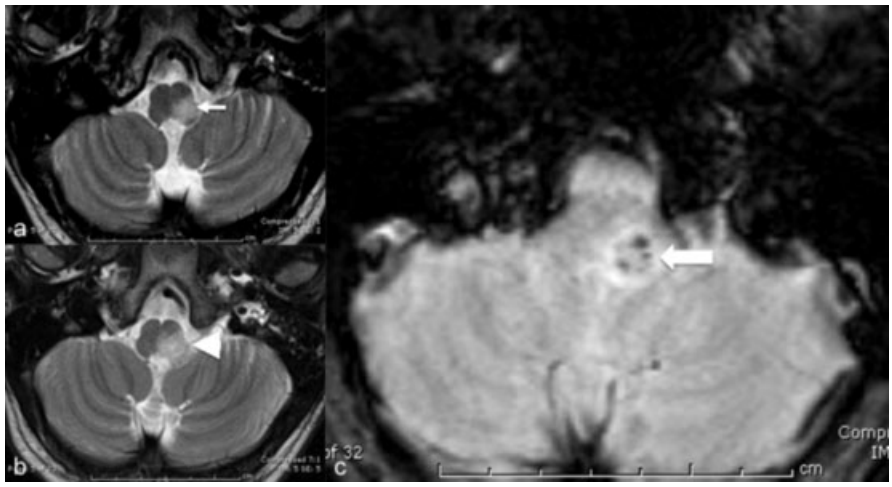

Fig 6. (A–C) Fifty-six-year-old male presenting with the clinical features of lateral medullary syndrome (Wallenberg's syndrome). (A) T2-weighted MRI revealing increased signal in the lateral medulla as expected in Wallenberg's syndrome (arrow). (B) T2-weighted image taken from a progress examination performed 6 weeks later. This reveals an expansion of the increased T2-signal raising concerns of low-grade tumor rather than infarction (arrowhead). (C) The corresponding SWI image from the progress scan revealing foci of susceptibility effect in the region of abnormal signal (block arrow). This reflects hemorrhagic transformation of infarction and was not present on the initial SWI MRI. The SWI sequence in this case greatly reinforced the diagnosis of infarct and prevented unnecessary interval imaging.

used is vital as the different systems produce contrary appearances (Table 1).

MRI systems are described, as being either left or right handed dependent on the direction of electric current within the electromagnet in relation to the direction of the magnetic field. The scanner used in our institution (Siemens) is a left-handed system. In this system, diamagnetic substances produce a negative phase shift leading to a loss of signal. This is displayed as a dark voxel. In contrast to this, paramagnetic substances produce a positive phase shift leading to increased signal. This is displayed as a bright voxel. The images produced therefore display calcium as dark signal and blood products/iron as high signal (see Figs 2 and 5). Right-handed systems produce the opposite effect with paramagnetic substances producing dark signal and diamagnetic substances a bright signal.[2,4,5]

Final SWI Images

The final SWI image (see Fig 3) displays both paramagnetic and diamagnetic substances as dark signal. This leads to excellent visualization of a number of structures. Deoxyhemoglobin leads to visualization of the cortical veins. Differing amounts of iron

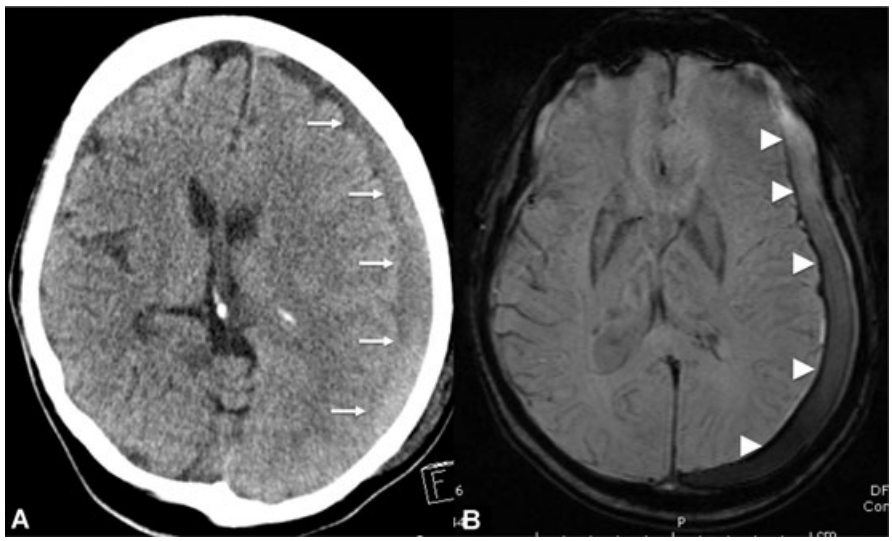

Fig 7. (A and B) Fifty-seven-year-old male presenting with recurrent falls. A mixed density subdural collection (arrows) in keeping with acute on chronic subdural hematoma is easily visualized on the unenhanced CT examination (A). The corresponding SWI image (B) elegantly outlines the subdural collection by demonstrating a low signal hemosiderin rim (arrowheads). The sensitivity of SWI for blood products may enable subdural hygromas to be readily distinguished from chronic subdural hematomas.

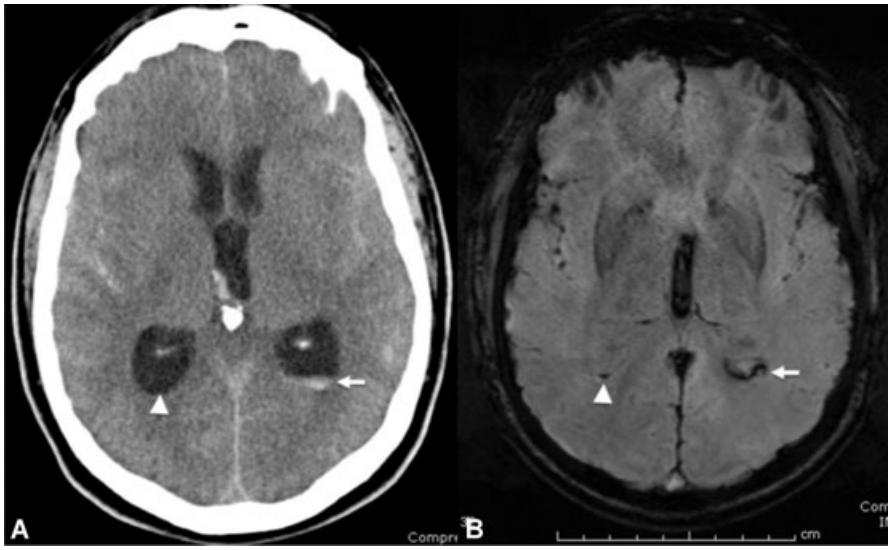

Fig 8. (A) An axial CT image revealing extensive subarachnoid haemorrhage filling the cerebral sulci along with blood layering in the left lateral ventricle (arrow). (B) The corresponding SWI axial image performed as part of an examination to try and determine the underlying cause of hemorrhage. Low signal susceptibility effect is seen in the posterior horn of the left lateral ventricle corresponding to the hemorrhage detected on CT (arrow). In addition, a further area of susceptibility effect is seen in the right lateral ventricle (arrowhead) indicating hemorrhage not readily identified on the CT examination.

deposition within the deep gray matter nuclei of the basal ganglia and particularly the dentate nucleus, red nucleus, and pars compacta of the substantia nigra allow easy identification. The imaging parameters of the GRE sequence used leads to low contrast between the remainder of the brain and cerebrospinal fluid (CSF). This allows greater contrast between areas of susceptibility and normal adjacent structures along with fluid attenuated inversion recovery (FLAIR)-like contrast in pathological areas of increased T2 signal. Fat and gas are also demonstrated as low signal. Dephasing artefact due to gas in the frontal sinuses leads to reduction of image quality in this region.

Scanning Technique

Imaging was performed on a 1.5 T SIEMENS MAGNETOM Symphony Tim syngo MR B15 (Siemens, Erlangen, Germany). Imaging parameters are as follows; T2 SWI 3-dimensional Axial Sequence, Slices per slab 32, field of view (FOV) read 230 mm, FOV phase 81.3%, Slice thickness 4.00 mm, TR 55 ms, TE 40.0 ms. The additional scanning time is approximately 3 minutes with automated image display produced by the main MRI workstation and then sent to the local Picture Archiving and Communication Systems (PACS) as a separate phase,

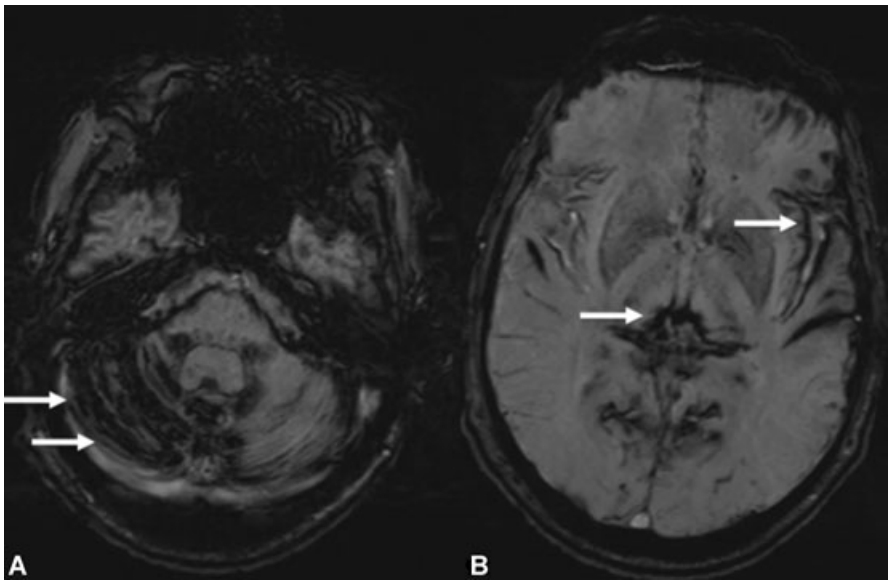

Fig 9. (A and B) Axial SWI images revealing low signal susceptibility representing hemosiderin deposition in a patient with the clinical presentation of superficial siderosis syndrome.

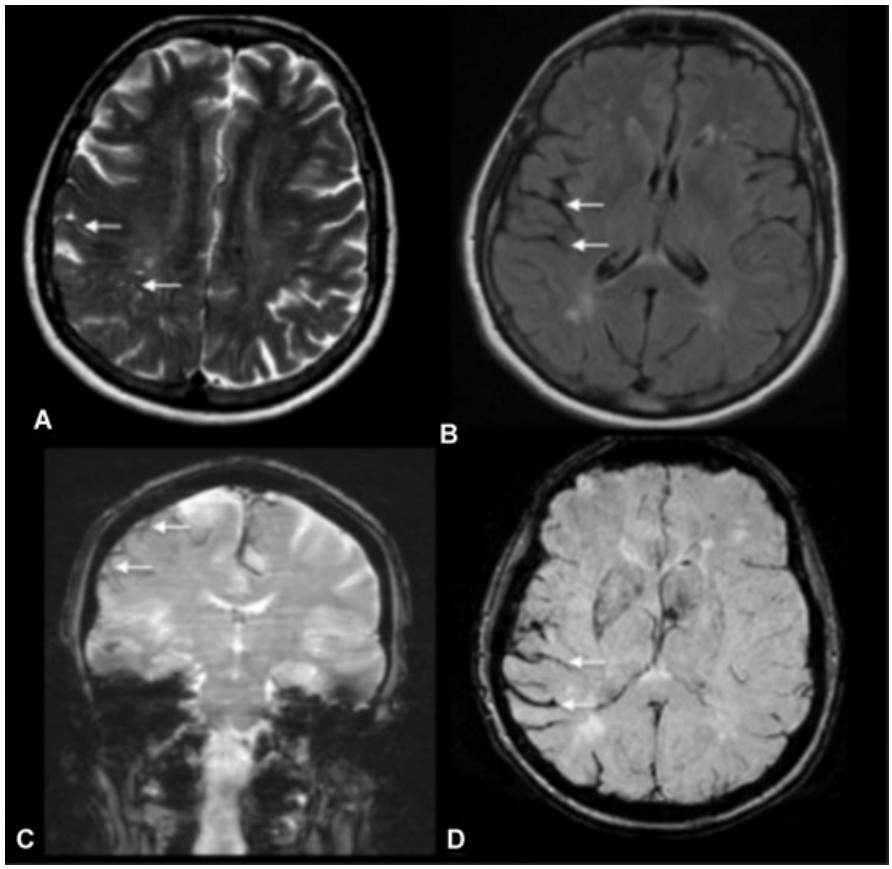

Fig 10. (A–D) Reveal superficial hemosiderin deposition in a patient with repeated head trauma. (A) (T2 axial), (B) (FLAIR axial), (C) ($T2^{*}$ coronal) and (D) (SWI) all reveal the characteristic low signal subpial coating to the brain. The findings are, however, most conspicuous on the SWI sequence. This suggests that SWI is the most sensitive sequence to date for detection of superficial siderosis.

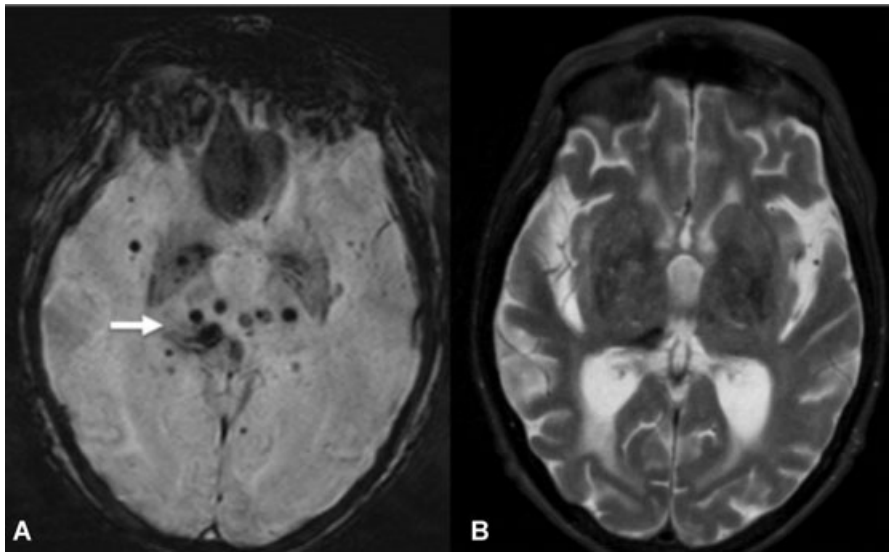

Fig 11. (A) An SWI image from the MRI examination performed as part of a stroke workup. It reveals multiple microheomorrhages in the basal ganglia (arrow) and deep white matter of the right temporal lobe. This indicated multiple hemorrhagic lacunar infarctions and is suggestive of hypertensive disease. (B) The corresponding T2 axial images revealing areas of increased signal in the same distribution although the presence of hemorrhage can not be demonstrated.

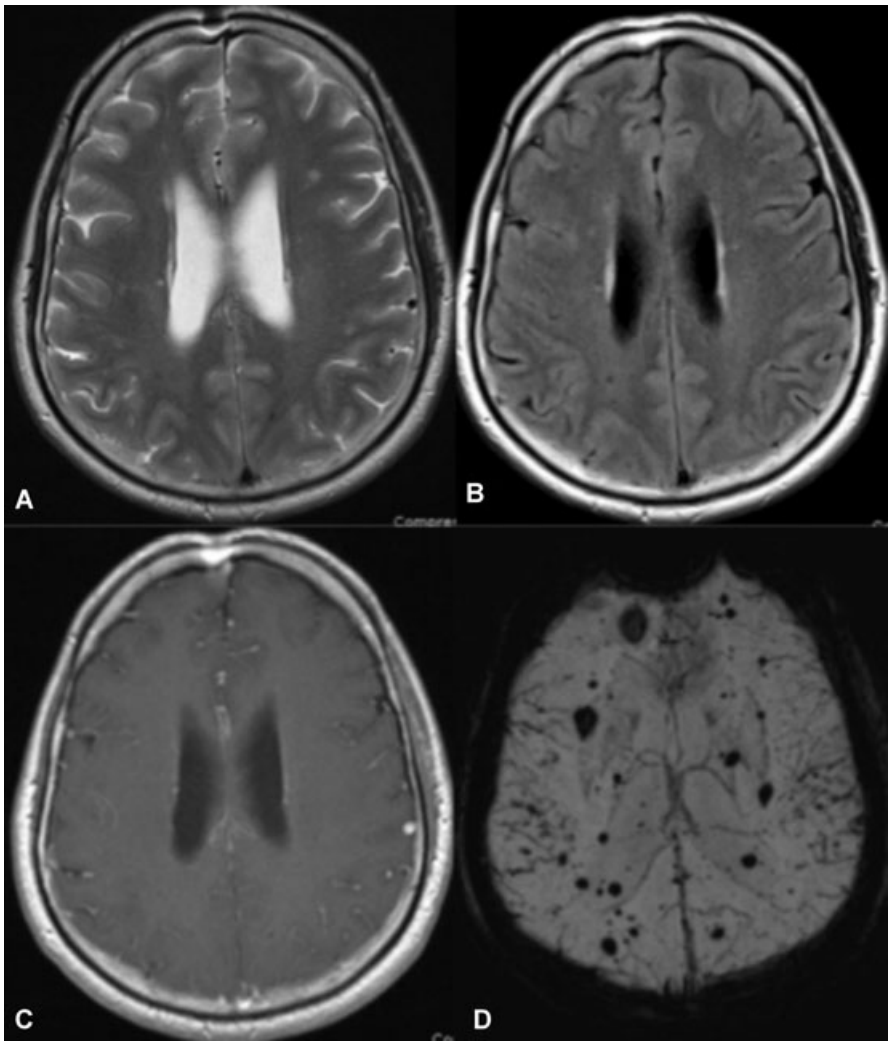

Fig. 12. (A–D) Taken from a patient presenting with intracranial hemorrhage. An MRI examination was performed to try and determine the underlying cause. Little abnormality was demonstrated on the T2 (A), FLAIR (B), and T1 postcontrast (C). (D)The corresponding SWI image revealing multiple foci of susceptibility effect in keeping with multiple cavernomas.

magnitude, and SWI image sequence. Imaging can also be performed in coronal and sagittal planes.

Results

Traumatic Brain Injury

One area in which SWI has shown definite diagnostic benefit is when imaging TBI. The exquisite sensitivity of SWI for detection of a small amount of hemorrhage has enabled information to be given to the referring clinicians with greater specificity (see Fig 4) revealing the full extent of diffuse axonal injury (DAI). TBI is also one area in which evidence exists in the literature to suggest greater sensitivity over T2*-weighted imaging.[6,7] It has also been suggested that prognostic information may be inferred from the volume of cerebral hemorrhage identified. A recent study has suggested that SWI is the most sensitive sequence for detection of traumatic hemorrhage, however; prognostic ability remains as yet unproven.[8] Number and volume of hemorrhagic lesions on SWI has also been shown to correlate with neuropsychiatric outcomes in pediatric patients.[9] SWI can detect brainstem hemorrhage that has obvious prognostic implications and is extremely difficult to accurately detect on computed tomography (CT). Subdural and subarachnoid hemorrhage (SAH) can also be demonstrated.

Cerebrovascular Disease

The sensitivity of SWI for detection of blood products gives potential for use across the spectrum of CVD. We have detected intravascular thrombus and hemorrhagic transformation in acute stroke, intracranial hemorrhage, cerebral microhemorrhage, vascular malformations, and venous thrombosis. We see great potential of this sequence for in situ thrombus imaging. This sequence can certainly be of immense help in stroke management than T2* in thrombus imaging as SWI has exquisite sensitivity in detecting deoxyhemoglobin seen in thrombi. Deoxyhemoglobin is paramagnetic and seen has low signal on SW images. Accurate location of the thromboemboli in the arteries may influence the neurointervetional techniques.

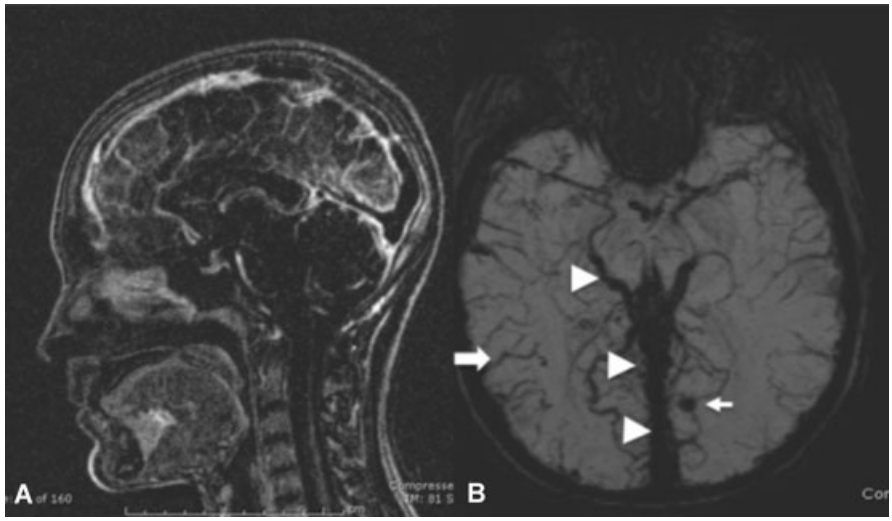

Fig 13. (A) Contrast-enhanced T1 BLADE MR venogram reveals extensive venous sinus thrombosis (VST). (B) A selected axial image from the corresponding SWI sequence. The diagnosis of VST can be readily made with current imaging sequences. Increased concentration of deoxyhemoglobin due to venous stasis leads to a prominent appearance of the venous sinuses, deep venous system (arrowheads), and cortical veins. This case highlights the exquisite detail revealed by SWI of the engorged cortical veins (block arrow) along with detection of microhemorrhage (arrow) due to venous infarction.

Stroke

Acute stroke caused by atherosclerotic thrombosis or thrombotic embolus is a common clinical occurrence optimally investigated by multimodality imaging. This includes CT, CT perfusion, and various MRI sequences including MR angiography. SWI augments current MR sequences in a number of situations. The exquisite sensitivity for blood products has enabled detection of in situ arterial thrombus (see Fig 5), hemorrhagic transformation demonstrated in smaller amounts than seen with CT, and has enabled diagnosis of infarction to be made in a case with concerns regarding the presence of low-grade malignancy (see Fig 6). As demonstrated in Figure 6, a 6-week follow-up scan shows a hemorrhagic transformation of infarct not seen on T2 W images but elegantly shown on SWI, this reinforces diagnosis of infarct over a neoplasm as the blooming effect was not seen on initial MRI confirming hemorrhagic transformation. It is unknown if the detection of such small amounts of hemorrhage should influence clinical management but it is suggested that this along with the detection of previous microhemorrhage may identify patients with an inherent vascular vulnerability and consequent increased risk of hemorrhage or recurrent stroke.[10]

SWI is also able to demonstrate a region of hypoperfusion. Hypoperfusion leads to increased deoxyhemoglobin relative to oxyhemoglobin in tissue capillaries and draining veins. This increased susceptibility difference produces a prominent hypointense signal on SWI within the draining veins of the underperfused territory.[11]

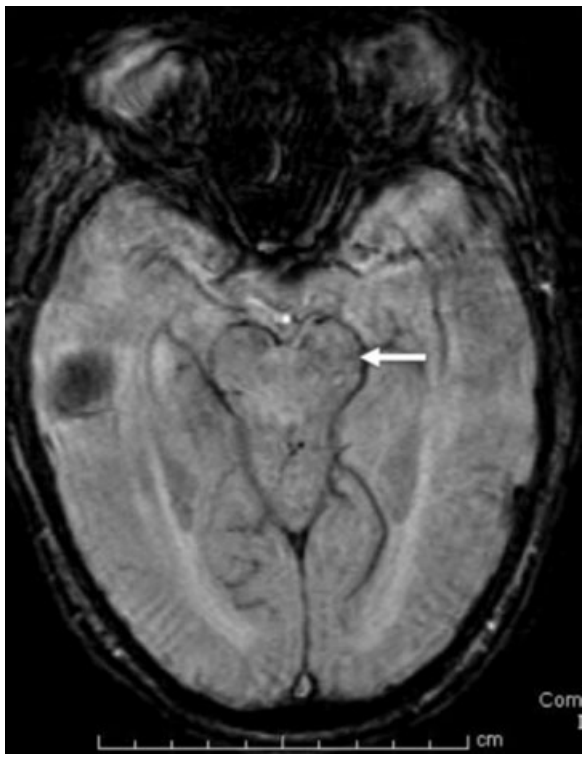

Fig 14. A selected axial SWI image from a 77-year-old male with a clinically suspected Parkinsonian syndrome. This reveals a marked decrease in iron content in the substantia nigra (arrow) reflected by a reduction in susceptibility artefact (compare this to the control subject in Fig 3). This suggests gliosis rather than iron deposition and may offer a way of distinguishing Parkinson's disease from Parkinson's Plus syndromes.

Intracranial Hemorrhage

CT Remains the mainstay for detection of intracranial hemorrhage, however, our experience has suggested that SWI offers advantages over CT in certain situations like,

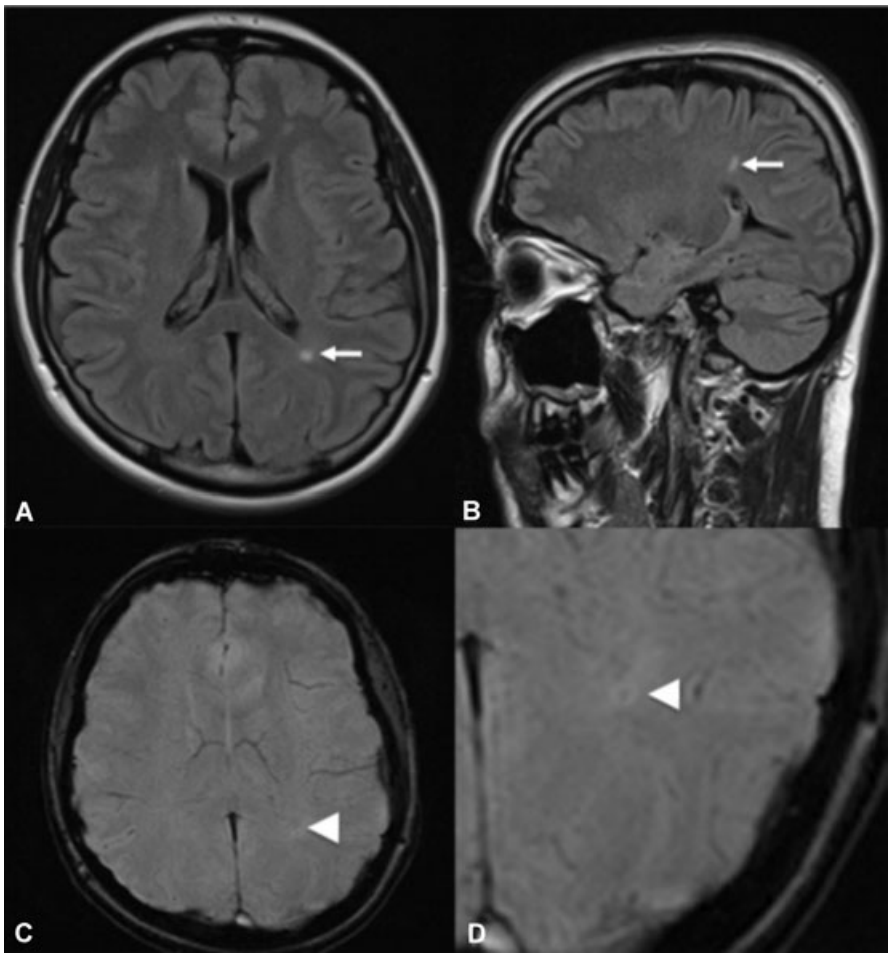

Fig 15. (A–D) Forty-two-year-old female presenting with an attack of optic neuritis. MRI was performed to look for evidence of MS. (A and B) FLAIR images revealing a high signal lesion in the left occipital deep white matter. This has a characteristic ovoid shape in a periventricular distribution consistent with an MS plaque (arrows). (C) The corresponding axial SWI image. This along with (D) (Magnified area of interest) reveals subtle decreased signal in the high signal lesion corresponding to increased susceptibility and iron deposition. This may suggest a chronic plaque.

Subdural Hemorrhage

SWI has the capability to distinguish blood products within a subdural hematoma (SDH) and may offer a niche in aging of SDH. The diagnosis of SDH is usually straightforward using CT. Limitations exist in detecting small volume hemorrhage, pediatric patients and differentiating chronic hematomas from subdural hygromas. SWI is able to demonstrate SDH and hemosiderin deposition around a fluid collection allows differentiation of a chronic SDH over a subdural hygroma (see Fig 7).

Subarachnoid Hemorrhage

Detection of subarachnoid hemorrhage (SAH) via imaging relies on CT. Although we do not use SWI for detection of SAH observations in a number of cases suggest it may offer a high sensitivity for its detection especially in the ventricular system. Figure 8 illustrates the presence of SAH in the posterior horn of the right lateral ventricle not demonstrated on an earlier CT examination.

Superficial Siderosis

FLAIR- and T2-weighted sequences offer the most reliable method of detecting subpial hemosiderin deposition seen in the superficial siderosis syndrome. This is demonstrated as a low signal coating to structure in contact with CSF. Figure 9 is taken from a patient with superficial siderosis syndrome. Hemosiderin deposition is demonstrated on the T2, FLAIR, and T2* sequences but is even more conspicuous on SWI. We have also identified multiple cases of localized cerebral hemosiderin deposition using SWI, which has not, or been less readily visualized using other MR sequences (see Fig 10). This suggests SWI is the most sensitive sequence for detection of subpial hemosiderin deposition. SWI may improve sensitivity of this condition although imaging of the cranial nerves and areas around the brainstem is limited due to susceptibility artifact

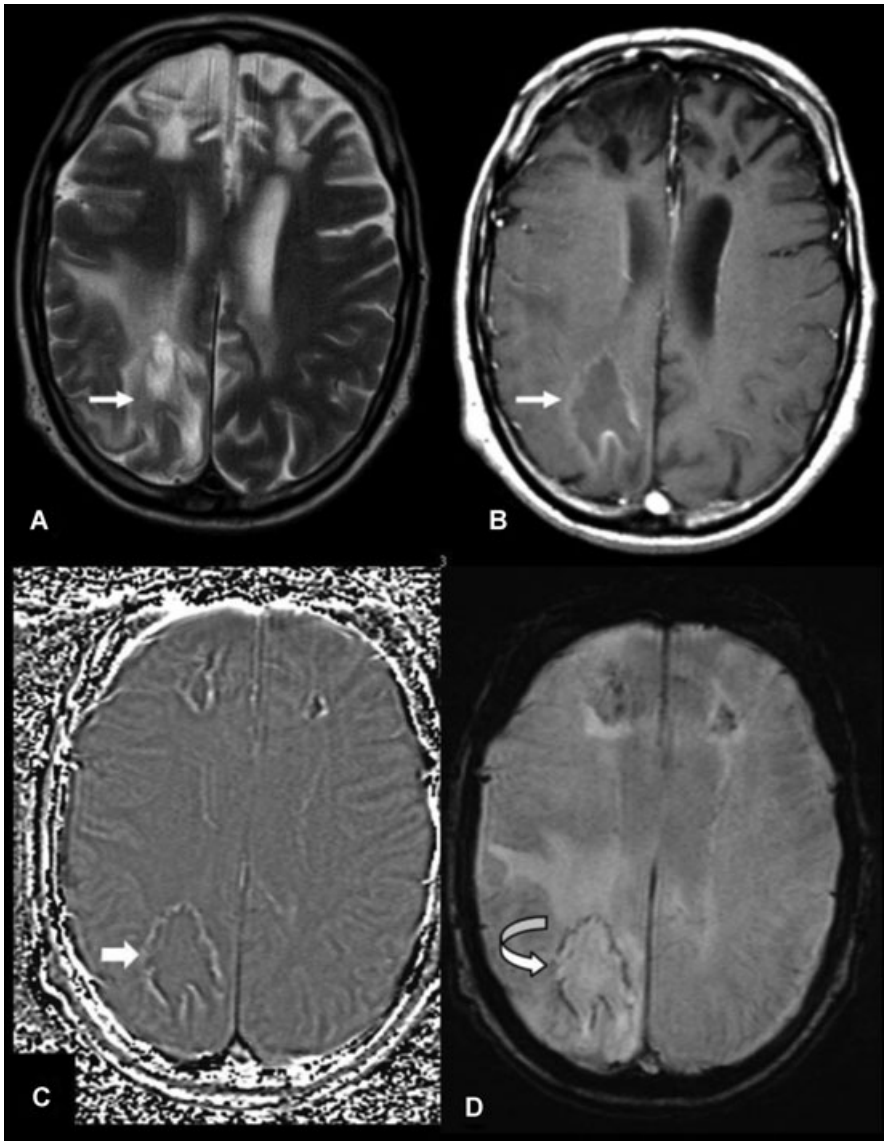

Fig 16. Taken from a patient with tumefactive MS. (A) (T2) and (B) (T1 postgadolinium) reveal a high signal lesion with peripheral enhancement (arrows) and extensive surrounding oedema. (C) (Phase) and (D) (SWI) demonstrate peripheral susceptibility rim (curved arrows) indicating a paramagnetic substance (old gliotic lesions are seen in the frontal lobes bilaterally).

caused by the proximity to the skull. The use of coronal SWI imaging may offer reduction of skull base artifact and improve imaging in this region.

Cerebral Microhemorrhage

SWI is exquisitely sensitive for cerebral microhemorrhage with proven improved sensitivity over other techniques including T2* gradient echo imaging.[10,12,13] Microhemorrhages are observed in multiple disorders including cerebral amyloid angiopathy (CAA), chronic hypertension, cerebral autosomal dominant arteriopathy with subcortical infarcts and leukoencephalopathy and cerebral vasculitis. The distribution of microhemorrhage within the brain enables differentiation between the conditions (see Fig 11). The sensitivity of SWI may enable earlier diagnosis along with assessment of severity and disease progression. Profound benefits can be inferred from more accurate assessment of these conditions, earlier diagnosis and more accurate assessment of a condition often aids in improving knowledge of a disease process enabling more effective management to be developed.

Vascular Malformations

Developmental venous anomalies (DVA), cavernomas, venous angiomas, and telangiectasias are lesions that contain low velocity and multidirectional flow. They are important clinically due to their propensity for hemorrhage. DVAs are less well imaged with conventional MRI sequences. Lesions have variable appearances depending on the presence of calcification or hemorrhage. Spin echo imaging is most sensitive for high flow and may not detect low flow. Time of flight angiography

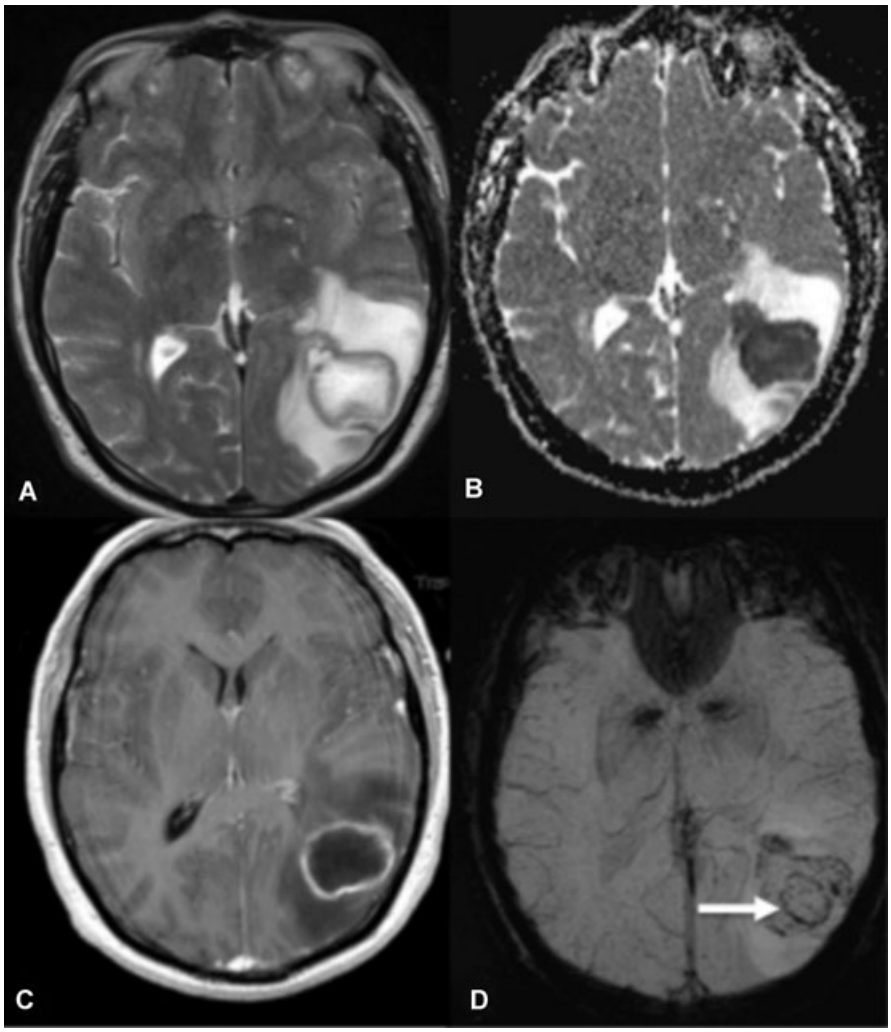

Fig 17. (A–D) Taken from an examination performed on a 44-year-old male who presented with headache and sepsis. The diagnosis of cerebral abscess can be made from the detection of a ring enhancing (C,T1 Post Gad), cystic structure (A) T2 with restricted diffusion (B). (D) The corresponding SWI image. This demonstrates peripheral low signal susceptibility effect (arrows) along with further internal ring of low signal and perilesional oedema.

is less sensitive due to multidirectional flow and low flow often demonstrates little enhancement following gadolinium. Literature evidence exists for SWI offering improved sensitivity over other sequences for detection of cavernomas,[14,15] this is consistent with our experience and Figure 12 demonstrates the extreme sensitivity of SWI. Improving the accuracy of lesion detection enables better treatment planning and determination of prognosis especially when lesions are seen in eloquent areas of the brain. SWI is also extremely sensitive for exclusion of lesion multiplicity.

Cerebral Venous Thrombosis

The diagnosis of VST is readily made with current MRI sequences. Cortical venous thrombosis is less common than dural sinus thrombosis and less readily diagnosed clinically or with neuroimaging. The variability seen in the number and position of cortical veins as well as the changing appearance of thrombus on T1- and T2-weighted sequences leads to limited exclusion. Neuroimaging therefore relies on both direct (such as visualization of thrombus) and indirect (localized hemorhage or venous infarction) signs.[16,17] Figure 13 is taken from a patient with extensive dural sinus thrombosis. The SWI sequence exquisitely demonstrates the congested venous architecture along with associated microhemorrhages due to venous infarction. SWI may offer an extremely useful adjunct to other sequences for detection of localized thrombosis by demonstrating the engorged thrombus filled vein as well as congestion in the draining territory.

Neurodegenerative Disease

Variations in cerebral iron content have been demonstrated on histopathology in a number of different neurodegenerative conditions.[18] These include Parkinson's disease and Parkinson plus syndromes, Huntington's disease, Alzheimer's, disease, amyotrophic lateral sclerosis, neurodegeneration with brain iron accumulation with and without and pantothenate kinase

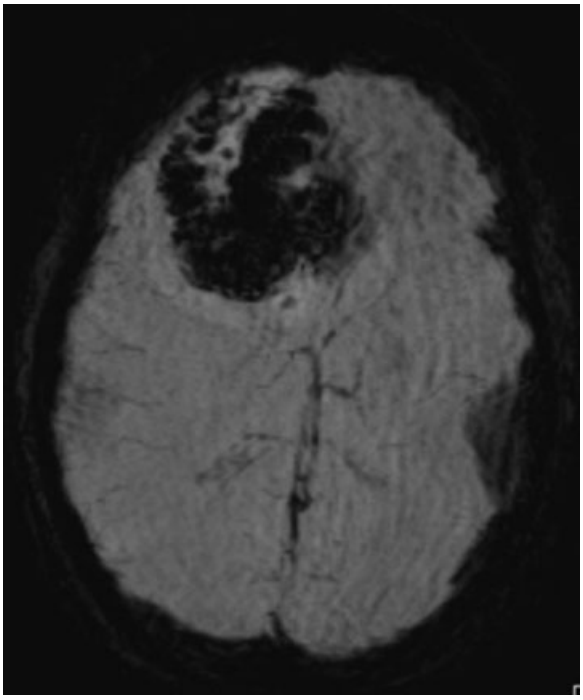

Fig 18. Demonstrates extensive low signal susceptibility effect in the right frontal lobe. This corresponds to hemosiderin deposition throughout a predominately solid tumor confirmed histologically as glioblastoma multiforme . A small amount of perilesional oedema is seen as a slightly higher signal than the surrounding normal brain.

associated neurodegeneration mutations.[19] Figure 14 demonstrates a study in which decreased substantia nigra iron content was demonstrated in a case of suspected Parkinson's plus syndrome. Unfortunately, normal cerebral iron distribution and quantification on SWI is not yet known making accurate interpretation of appearances difficult. This appearance suggests a Parkinson's plus syndrome rather than Parkinson's disease in which increased iron would be suspected.[20] This particular feature may help in differentiating classic Parkinson's disease from Parkinson's plus syndrome.

The sensitivity of SWI for the susceptibility effect of iron enables structures such as the dentate nucleus and pars compacta of the substantia nigra along with basal ganglia structures much more conspicuous than in other available techniques (see Fig 2). If quantification of the normal iron distribution in these structures can be established, in future SWI may offer an exciting prospect for research and may offer increased sensitivity and specificity for iron detection, ability to monitor treatment progress, and assessment of disease severity in neurodegenerative conditions.

Demyelination

Demyelination is extremely well demonstrated by MRI with a reliance on FLAIR sequences. SWI may offer additional information to current routine sequences improving sensitivity and offering further understanding of the disease process based upon intralesional iron deposition. The ability of SWI for small vein depiction enables perivenous distribution of multiple sclerosis (MS) plaques to be observed along with low signal intralesional iron deposition, which can be central (see Fig 15) or ring like in nature. The significance of the different types of lesion is yet to be established.[21] Intralesional iron deposition may indicate chronicity offering potential for more accurate plaque burden assessment and monitoring of disease activity.

One interesting potential application for SWI is to aid in differentiation of tumefactive demyelination from neoplasia. Kim et al[22] suggest that the presence of intralesional susceptibility signals exclude nonneoplastic conditions including tumefactive MS. Our experience of this pathology is slightly different demonstrating a peripheral rim of low signal susceptibility signal (see Fig 16). Hemorrhage is not demonstrated in demyelination and therefore the peripheral rim of susceptibility signal is thought analogous to free radicals seen in abscesses. As discussed below, these are produced by macrophages at the periphery of an active lesion.

Infection

SWI has no current role in the imaging of cerebral infection. It may demonstrate calcification in fungal infections, however, this can be achieved with CT. Observations in our practice

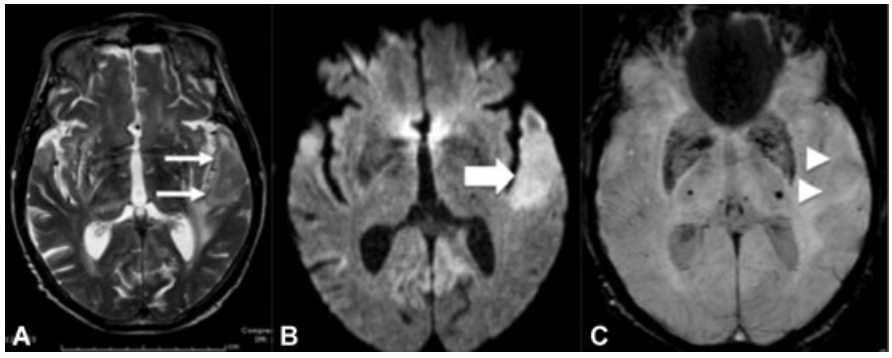

Fig 19. (A–C) Taken from a study performed on a 73-year-old female who presented with acute confusional state. (A) An axial T2 image revealing increased signal (arrows) in the left temporal lobe with surrounding vasogenic oedema. This area showed enhancement following gadolinium (not shown) and restricted diffusion (B). Biopsy later confirmed diagnosis of lymphoma. (D) The corresponding SWI sequence, which reveals the oedema but no areas of susceptibility effect to suggest hemorrhage/necrosis.

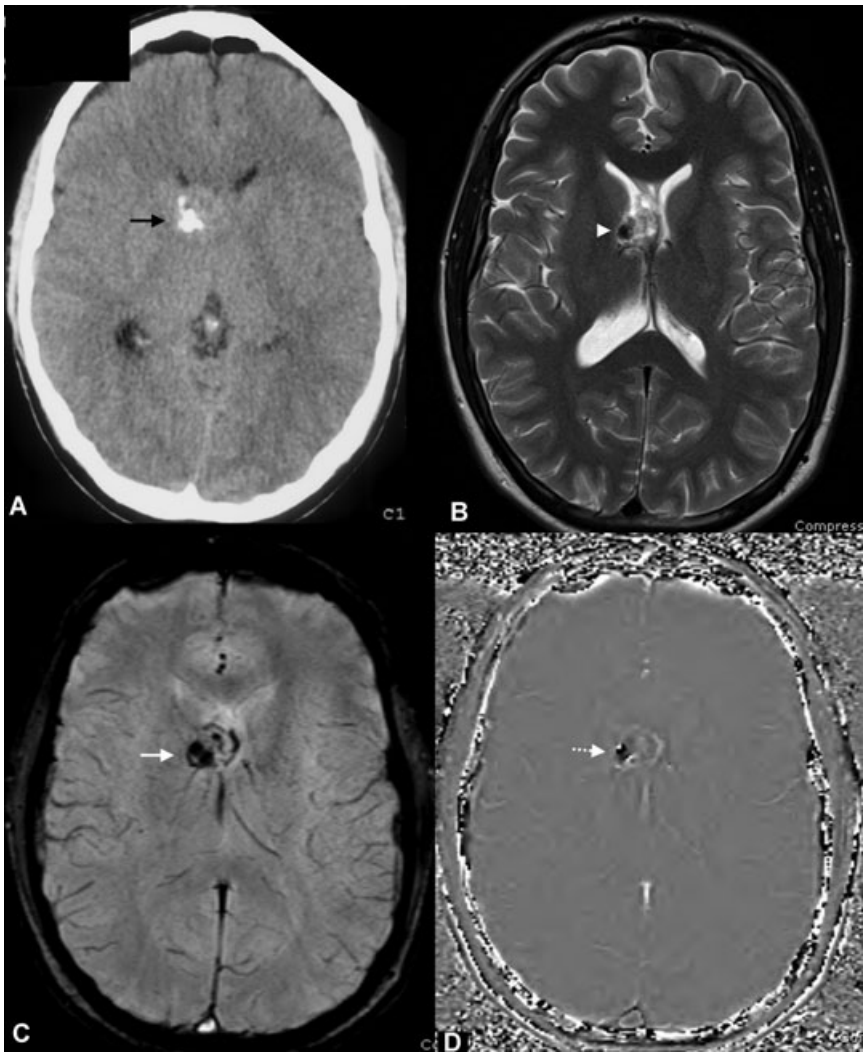

Fig 20. (A) (Unenhanced CT), (B) (axial T2), (C) (SWI), and (D) (Phase) are taken from a patient with a subependymal giant cell astrocytoma. Low signal is seen on T2 (arrowhead) along with low susceptibility signal on the SWI sequence (white arrow). The phase image confirms the presence of diamagnetic calcification as low signal (dashed arrow) and not hemosiderin. This is corroborated by the CT examination (black arrow). Incidental pneumocephalus post-biopsy.

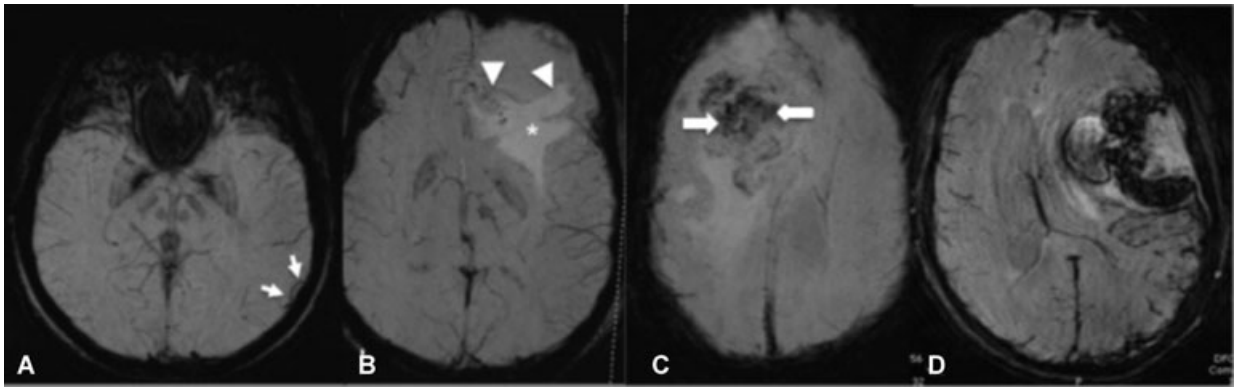

Fig 21. (A–D) All axial SWI images in cases of biopsy-proven meningioma. (A) Reveals a small left temporal meningioma. Veins surrounding are displaced by the mass (arrows). (B) Identifies a large left frontal meningioma. This has a uniform internal structure but the dilated surrounding veins are again visualized (arrowheads) with adjacent oedema (asterisk). (C) Demonstrates the surrounding veins and oedema as in the other examples. It also demonstrates low signal susceptibility effect in the mass relating to hemorrhage or calcification (block arrows). (D) An extreme example revealing extensive susceptibility effect within a Grade II meninigioma. As in the other cases, surrounding veins and peritumoral oedema are demonstrated.

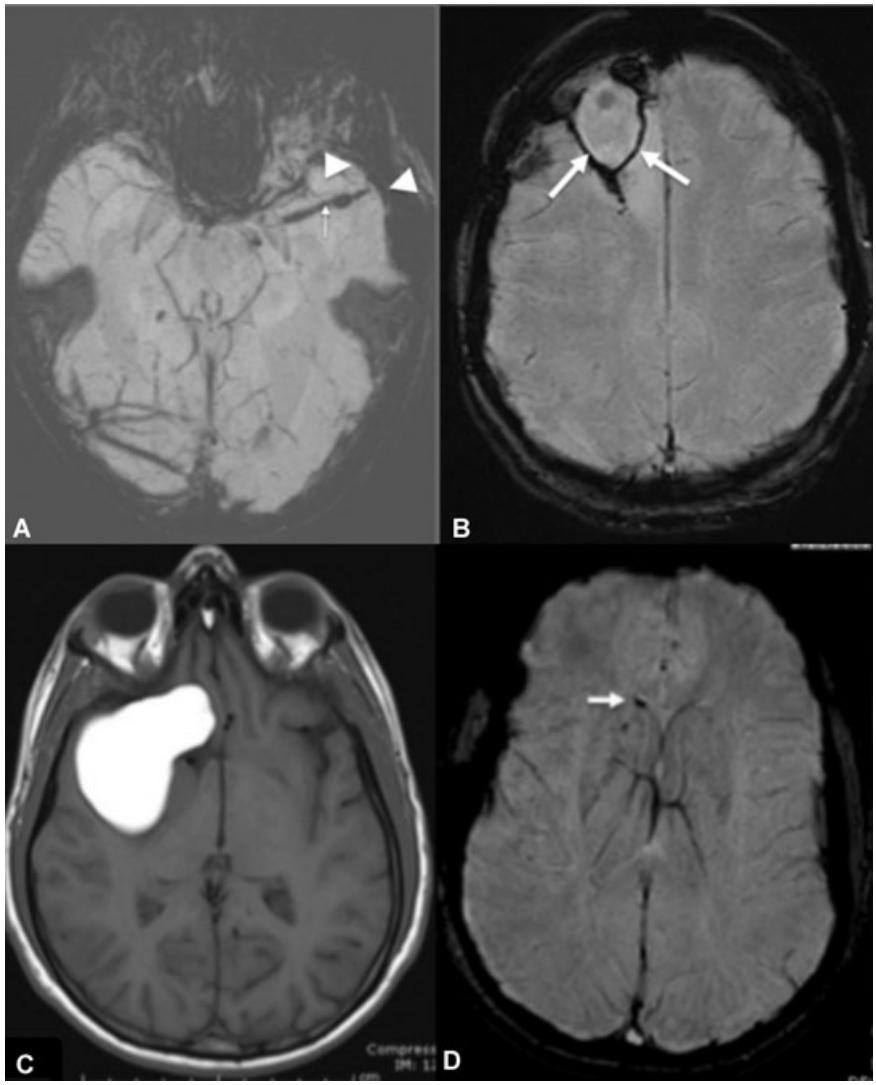

Fig 22. (A and B) Axial SWI images. (A) Reveals linear low signal in the left temporal lobe on this SWI image (arrow). This is caused by hemosiderin deposition along a biopsy tract. In addition, a small subdural hematoma is demonstrated (arrowheads). (B) Reveals oval-shaped low signal on this SWI image. This corresponds to circumferential hemosiderin deposition in a postoperative cavity in the right frontal lobe (arrows). (C) (T1) and (D) (SWI) are taken from a patient with a dermoid tumor. (C) Reveals a large fat density mass. (B) Reveals a small focus of susceptibility effect lying nondependently within the right lateral ventricle (arrow). This corresponds to intraventricular fat.

have shown a low signal rim of susceptibility effect in cerebral abscesses (see Fig 17). As with other gradient echo imaging, we believe this represents paramagnetic free radicals within phagocytosing macrophages at the periphery of the abscess. This rim resolves following treatment due to a reduction of phagocytic activity.[23] SWI may therefore offer a method of assessing treatment response.

Neoplasia

The characterization of cerebral mass lesions is dependent on many factors including anatomical location, clinical presentation, patient age, and appearances on different MRI sequences. SWI can be used to improve diagnostic specificity and aid in management planning. The presence of extensive susceptibility effect and susceptibility conglomerates within a lesion suggests vascular proliferation and has been shown to correlate with pathologically proven high-grade lesions.[22,24] This has also been a consistent finding in our practice with glioblastoma multiforme (GBM) (see Fig 18). In contrast, lymphoma rarely shows hemorrhage,[22,25] which has enabled the diagnosis to be favored prior to confirmatory biopsy (see Fig 19). The differentiation of diffusely infiltrating GBM and lymphoma is important as management and prognosis is vastly different.

Gliosarcomas show dural enhancement due to their peripheral location and dural invasion. Observations suggest that GBM demonstrates more heterogeneity and susceptibility effect on SWI, which may aid in lesion differentiation of the 2 tumor types.

The ability to distinguish between the different tumor types with imaging may negate the need for biopsy in some patients. The presence of vascular proliferation indicates a World Health Organization grade IV tumor. This is not necessarily uniform

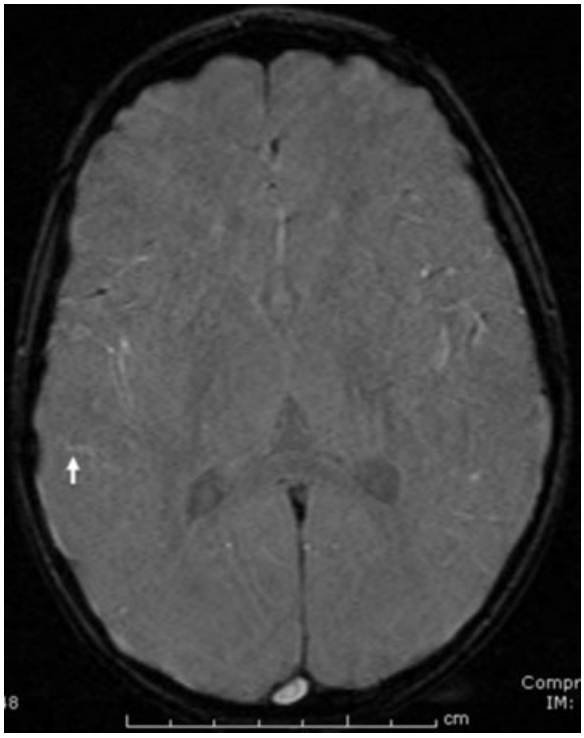

Fig 23. An axial SWI image taken from a patient under general anesthesia. This demonstrated attenuation of normal low signal cortical veins along with areas of increased venous signal (arrow).

throughout a tumor therefore the presence of susceptibility effect could be used as a guide for surgical biopsy.

Low-grade lesions are less likely to show susceptibility effect, however, the presence of calcification must be distinguished by reviewing the phase sequences (see Fig 20). In our limited experience with meningiomas, SWI has shown varying results with no direct correlation with susceptibility effect and tumor grade. This may be due to small foci of calcification within the tumors. As expected, the majority of these tumors show no susceptibility effect (see Fig 21). Figure 21D is an SWI image from a patient with a pathologically proven meningioma. Extensive low signal susceptibility changes similar to those seen in GBM are visible. Unfortunately, phase imaging was not recorded separately at the time of imaging so correlation with calcification was not possible in this case. Careful analysis for displacement of vessels around the mass is necessary to establish its extraxial location. The depiction of veins/vessels surrounding a mass may enable determination of intra- or extraaxial origins in challenging cases.

Miscellaneous

Susceptibility effect can also be seen in other situations especially postoperatively and must not be confused with pathological processes. Pneumocephalus, intraventricular fat, postoperative parenchymal, and extraxial hemosiderin deposition will all reveal susceptibility effect (see Fig 22). Correlation with the clinical scenario and other sequences is therefore necessary for accurate characterization.

SWI of Brain and General Anesthesia

An interesting observation is seen in patients undergoing general anesthesia for MRI. Normal veins on SWI images appear dark and are seen in extreme details whereas under general anesthetic the cortical veins appear attenuated and/or have bright signal (Fig 23). This has been postulated to represent a response to a decreased rate of oxygen extraction related to the depth of anesthesia.[26] This effect may enable differentiation of veins from hemorrhage.

Conclusion

We have found SWI to offer additional information over and above routine imaging sequences. SWI is therefore now incorporated into our routine neuroimaging protocols. Establishing SWI as a routine neuroimaging sequence will help to unlock its potential in many of the areas discussed above. The utility of SWI in thrombus imaging, tumor grading, TBI, cerebral infection, venous anatomy, Parkinson's plus syndromes, and particularly the ability to differentiate calcium and blood have exciting implications for research in pursuit of a greater understanding of neuropatholgical processes leading to improved diagnostic sensitivity and specificity. Imaging in multiple planes and the increasing use of higher field strength magnets may offer more accuracy and development of further clinical applications.

References

1. Mittal S, Wu Z, Neelavalli J, et al. Susceptibility-weighted imaging: technical aspects and clinical applications, part 2. *AJNR Am J Neuroradiol* 2009;30:232-252.
2. Thomas B, Somasundaram S, Thamburaj K, et al. Clinical applications of susceptibility weighted MR imaging of the brain – a pictorial review. *Neuroradiology* 2008;50:105-116.
3. Haacke EM, Mittal S, Wu Z, et al. Susceptibility-weighted imaging: technical aspects and clinical applications, part 1. *AJNR Am J Neuroradiol* 2009;30:19-30.
4. Wu Z, Mittal S, Kish K, et al. Identification of calcification with MRI using susceptibility-weighted imaging: a case study. *J Magn Reson Imaging* 2009;29:177-182.
5. Rauscher A, Sedlacik J, Barth M, et al. Magnetic susceptibility-weighted MR phase imaging of the human brain. *AJNR Am J Neuroradiol* 2005;26:736-742.
6. Tong KA, Ashwal S, Holshouser BA, et al. Diffuse axonal injury in children: clinical correlation with hemorrhagic lesions. *Ann Neurol* 2004;56:36-50.
7. Tong KA, Ashwal S, Holshouser BA, et al. Hemorrhagic shearing lesions in children and adolescents with posttraumatic diffuse axonal injury: improved detection and initial results. *Radiology* 2003;227:332-339.
8. Chastain CA, Oyoyo U, Zipperman M, et al. Predicting outcomes of traumatic brain injury by imaging modality and injury distribution. *J Neurotrauma* 2009;26:1183-1196.
9. Babikian T, Freier MC, Tong KA, et al. Susceptibility weighted imaging: neu-ropsychologic outcome and pediatric head injury. *Pediatr Neurol* 2005;33:184-194.
10. Gao T, Wang Y, Zhang Z. Silent cerebral microbleeds on susceptibility-weighted imaging of patients with ischemic stroke and leukoaraiosis. *Neurol Res* 2008;30:272-276.
11. Fushimi Y, Miki Y, Mori N, et al. Signal changes in the brain on susceptibility-weighted imaging under reduced cerebral blood flow: a preliminary study. *J Neuroimaging* 2009;20:255-259.
12. Ghostine S, Raghavan R, Khanlou N, et al. Cerebral amyloid angiopathy: micro-haemorrhages demonstrated by magnetic

resonance susceptibility-weighted imaging. *Neuropathol Appl Neurobiol* 2009;35:116-119.
13. Haacke EM, DelProposto ZS, Chaturvedi S, et al. Imaging cerebral amyloid angiopathy with susceptibility-weighted imaging. *AJNR Am J Neuroradiol* 2007;28:316-317.
14. de Souza JM, Domingues RC, Cruz LC, et al. Susceptibility-weighted imaging for the evaluation of patients with familial cerebral cavernous malformations: a comparison with t2-weighted fast spin-echo and gradient-echo sequences. *AJNR Am J Neuroradiol* 2008;29:154-158.
15. Cooper AD, Campeau NG, Meissner I. Susceptibility-weighted imaging in familial cerebral cavernous malformations. *Neurology* 2008;71:382.
16. Boukobza M, Crassard I, Bousser MG, et al. MR imaging features of isolated cortical vein thrombosis: diagnosis and follow-up. *AJNR Am J Neuroradiol* 2009;30:344-348.
17. Duncan IC, Fourie PA. Imaging of cerebral isolated cortical vein thrombosis. *Am J Roentgenology* 2005;184:1317-1319.
18. Drayer B, Burger P, Darwin R, et al. MRI of brain iron. *Am J Roentgenology* 1986;147:103-110.
19. Hayflick SJ, Hartman M, Coryell J, et al. Brain MRI in neurodegeneration with brain iron accumulation with and without PANK2 mutations. *AJNR Am J Neuroradiol* 2006;27:1230-1233.
20. Adachi M, Hosoya T, Haku T, et al. Evaluation of the substantia nigra in patients with Parkinsonian syndrome accomplished using multishot diffusion-weighted MR imaging. *AJNR Am J Neuroradiol* 1999;20:1500-1506.
21. Haacke EM, Makki M, Ge Y, et al. Characterizing iron deposition in multiple sclerosis lesions using susceptibility weighted imaging. *J Magn Reson Imaging* 2009;29:537-544.
22. Kim HS, Jahng G-H, Ryu CW, et al. Added value and diagnostic performance of intratumoral susceptibility signals in the differential diagnosis of solitary enhancing brain lesions: preliminary study. *AJNR Am J Neuroradiol* 2009. [Epub ahead of print].
23. Haimes AB, Zimmerman RD, Morgello S, et al. MR imaging of brain abscesses. *AJR Am J Roentgenol* 1989;152:1073-1085.
24. Pinker K, Noebauer-Huhmann IM, Stavrou I, et al. High-resolution contrast-enhanced, susceptibility-weighted MR imaging at 3T in patients with brain tumors: correlation with positron-emission tomography and histopathologic findings. *AJNR Am J Neuroradiol* 2007;28:1280-1286.
25. Erdag N, Bhorade RM, Alberico RA, et al. Primary lymphoma of the central nervous system: typical and atypical CT and MR imaging appearances. *Am J Roentgenology* 2001;176:1319-1326.
26. Kesavadas C, Thomas B, Misra S, et al. Attenuation of cerebral veins in susceptibility-weighted MR imaging performed with the patient under general anesthesia. *AJNR Am J Neuroradiol* 2008;29:e71.